Scientific
Research

Synthesis and Characterization of Co_3O_4 Thin Film

Vikas Patil[1*], Pradeep Joshi[1], Manik Chougule[1], Shashwati Sen[2]

[1]Materials Research Laboratory, School of Physical Sciences, Solapur University, Solapur, India; [2]Crystal Technology Section, Bhabha Atomic Research Centre, Mumbai, India.
Email: [*]drvbpatil@gmail.com

ABSTRACT

Nanosized Co_3O_4 thin films were prepared on glass substrates by using sol-gel spin coating technique. The effect of annealing temperature (400°C - 700°C) on structural, morphological, electrical and optical properties of Co_3O_4 thin films were studied by X-ray diffraction (XRD), Scanning Electron Microscopy (SEM), Electrical conductivity and UV-visible Spectroscopy (UV-Vis). XRD measurements show that all the films are nanocrystallized in the cubic spinel structure and present a random orientation. Six prominent peaks, corresponding to the (111) phase ($2\theta \approx 18.90°$), (220) phase ($2\theta \approx 31.29°$), (311) phase ($2\theta \approx 36.81°$), (222) phase ($2\theta \approx 38.54°$), (400) phase ($2\theta \approx 44.80°$), (511) phase ($2\theta \approx 59.37°$) and (440) phase ($2\theta \approx 65.27°$) appear on the diffractograms. The crystallite size increases with increasing annealing temperature. These modifications influence the optical properties. The morphology of the sol gel derived Co_3O_4 shows nanocrystalline grains with some overgrown clusters and it varies with annealing temperature. The optical band gap has been determined from the absorption coefficient. We found that the optical band gap energy decreases from 2.58 eV to 2.07 eV with increasing annealing temperature between 400°C - 700°C. These mean that the optical quality of Co_3O_4 films is improved by annealing. The dc electrical conductivity of Co_3O_4 thin films were increased from 10^{-4} to 10^{-2} $(\Omega \cdot cm)^{-1}$ with increase in annealing temperature. The electron carrier concentration (n) and mobility (μ) of Co_3O_4 films annealed at 400°C - 700°C were estimated to be of the order of 2.4 to 4.5 × 10^{19} cm^{-3} and 5.2 to 7.0 × 10^{-5} cm$^2 \cdot V^{-1} \cdot s^{-1}$ respectively. It is observed that Co_3O_4 thin film annealing at 700°C after deposition provide a smooth and flat texture suited for optoelectronic applications.

Keywords: Sol Gel Method; Structural Properties; Optical Properties; Electrical Properties

1. Introduction

Cobalt oxide is an important p-type semiconductor with direct optical band gaps at 1.48 and 2.19 eV [1], Co_3O_4 has been investigated extensively as promising materials in gas-sensing and solar energy absorption and as an effective catalyst in environmental purification and chemical engineering [2,3]. Co_3O_4 has a stable normal spinel structure of AB_2O_4 type; where Co^{2+} ions occupy the tetrahedral 8a sites and Co^{3+} occupy the octahedral 16d sites [4]. In addition, Co_3O_4 has been widely studied for its application as lithium ion battery electrodes, catalysts, ceramic pigments, field-emission materials and magnetic material [5-10].

According to the literature survey, the systematic investigations on viz effect of annealing on structural, morphology, electrical conductivity and band gap of nanocrystalline Co_3O_4 thin films by sol-gel spin coating method has been sparsely studied.

In the present investigations, efforts are taken to report new method of synthesis and characterization of nanocry-

stalline Co_3O_4 thin films by simple and inexpensive sol-gel spin coating technique and effect of annealing on their structure, morphology and optoelectronic properties.

2. Experimental Details

Nanosized Co_3O_4 thin films have been synthesized by a sol-gel spin coating technique using Cobalt acetate tetra hydrates as a source of Cobalt oxide. In a typical experiment; Cobalt acetate tetra hydrate was added to 40 ml of methanol and stirred vigorously at 60°C for 1 h, leading to the formation of light pink color powder. The as prepared powder was sintered at various temperatures ranging from 400°C - 700°C with a fixed annealing time of 1 h in an ambient air to obtain Co_3O_4 with different crystallite sizes. The nanocrystalline Co_3O_4 powder was further dissolved in *m*-cresol and solution was continuously stirred for 11 h at room temperature and filtered. The filtered solution was deposited on to a glass substrate by a single wafer spin processor (APEX Instruments, Kolkata, Model SCU 2007). After setting the substrate on the substrate holder of the spin coater, the coating solution (approxi-

---

mately 0.2 ml) was dropped and spin-casted at 3000 RPM for 40 s in an air and dried on a hot plate at 100°C for 10 min. **Figure 1** shows the flow diagram for the sol gel synthesis and deposition of Co_3O_4 films by spin-coating technique. The structural properties of the Co_3O_4 films were investigated by means of X-ray diffraction (XRD) (Philips PW-3710, Holland) using Cu K$_\alpha$ radiation ($\lambda = 1.5406$ Å). The surface morphology of the Co_3O_4films were examined by scanning electron microscopy (SEM) (Model JEOL-JSM-6360, Japan), operated at 20 kV. The dc electrical conductivity measurements of Co_3O_4 thin films were performed using four probe technique in 300 K - 500 K temperature range. The optical absorption spectra of the Co_3O_4 thin films were measured using a double-beam spectrophotometer Shimadzu UV-140 over 200 nm - 1000 nm wavelength range. The thickness of the film was measured by using weight difference method and Dektak profilometer.
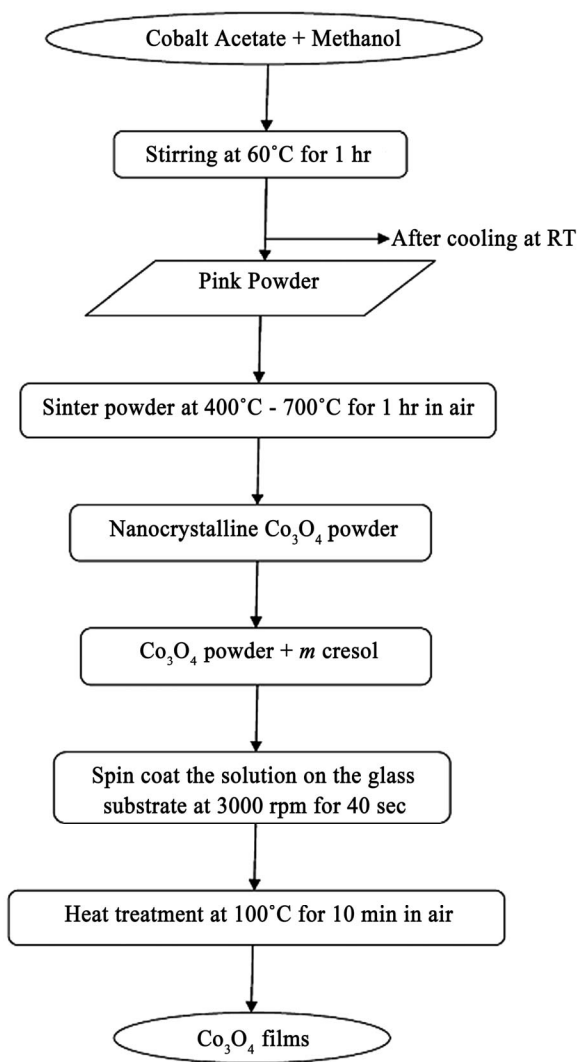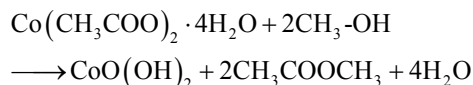

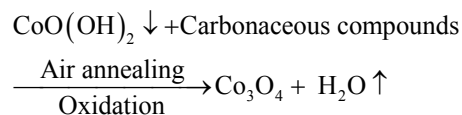**Figure 1. Flow diagram for Co_3O_4 films prepared from the sol-gel process using the spin-coating method.**

3. Results and Discussions

3.1. Growth Mechanism and Film Formation of Co_3O_4

The growth mechanism of Co_3O_4 film formation by the sol gel spin coating method can be enlightened as follows:

$$Co(CH_3COO)_2 \cdot 4H_2O + 2CH_3\text{-}OH$$
$$\longrightarrow CoO(OH)_2 + 2CH_3COOCH_3 + 4H_2O$$

Since to improve crystallinity and remove hydroxide phase, films were annealed for 1 h pure Co_3O_4 film is formed after air annealing by following mechanism:

$$CoO(OH)_2 \downarrow + \text{Carbonaceous compounds}$$
$$\xrightarrow[\text{Oxidation}]{\text{Air annealing}} Co_3O_4 + H_2O \uparrow$$

After annealing in air at temperatures (400°C - 700°C) the change in color was observed owing to the conversion of cobalt oxyhydroxide (CoOOH) into Co_3O_4 (dark black in color).

Thickness of Co_3O_4 was calculated by weight difference method using formula:

$$t = m/A\rho \tag{1}$$

where t is film thickness of the film; m is actual mass deposited onto substrate; A is area of the film and ρ is the density of cobalt oxide (6.2 g/cm^3).
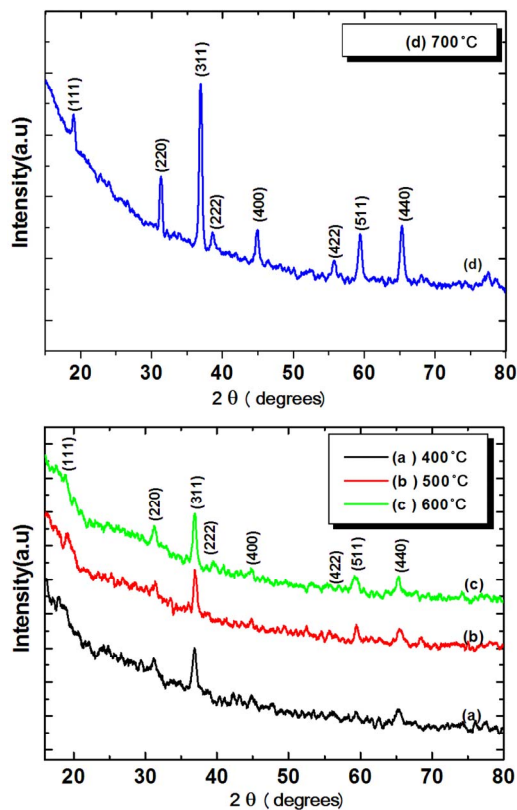
It was observed that increasing the annealing temperature (400°C - 700°C) resulted in a decrease in film thickness. The Co_3O_4 film thickness is also confirmed by Dektak profilometer and is nearly equal to weight difference method and is presented in **Table 1**.

3.2. Structural Analysis

Figure 2 shows X-ray diffraction patterns of Co_3O_4 thin films deposited on glass substrates by spin-coating at different annealing temperatures of 400°C, 500°C, 600°C, and 700°C. At 400°C - 600°C annealing, small peaks were observed and the film shows a poor crystallinity. Films annealed at temperature $\geq$600°C, exhibit sharp diffraction peaks characteristics of the Co_3O_4 cubic spinel structure. From **Figure 2**, (111) phase ($2\theta \approx 18.90°$), (220) phase ($2\theta \approx 31.29°$), (311) phase ($2\theta \approx 36.81°$), (222) phase($2\theta \approx 38.54°$) , (400) phase ($2\theta \approx 44.80°$), (511) phase ($2\theta \approx 59.37°$) and (440) phase ($2\theta \approx 65.27°$) XRD peaks were observed, and it is concluded that all the films were polycrystalline with a cubic spinel structure [JCPD: 78-1970, a = 8.02°A] and a random orientation, which generally occurs in the growth of Co_3O_4 thin films [11-13].The degree of c-axis orientation of the Co_3O_4 thin films was strongly dependent on the annealing temperature. It increases as the annealing temperature increases. The average particle sizes of Co_3O_4 thin film were calculated using the full width at

Table 1. Effect of annealing on Co$_3$O$_4$ thin film properties.

Sr. No.	Annealing temperature ˚C	Crystallite size nm (from XRD)	Thickness μm	Energy gap E$_g$, eV	Activation Energy, E$_{a\sigma}$, eV HT	LT	Carrier concentration, cm^{-3}	Mobility cm^2, V^{-1}·s^{-1}
1	400	53.40	0.7748	2.58	0.21	0.060	2.40×10^{19}	5.20×10^{-5}
2	500	58.25	0.6887	2.34	0.36	0.062	2.75×10^{19}	5.78×10^{-5}
3	600	64. 70	0.6425	2.21	0.48	0.064	3.27×10^{19}	6.45×10^{-5}
4	700	68.54	0.5998	2.07	0.54	0.064	4.50×10^{19}	7.00×10^{-5}

Figure 2. X ray diffraction patterns of Co$_3$O$_4$ films at different annealing temperatures.

half maximum (FWHM) of (311) peak from the Scherrer's method [Equation (2)] and are presented in **Table 1**.

$$D = C\lambda / \beta \cos\theta \qquad (2)$$

where β is the full width at half maximum of X-ray peak in radians, D is the crystallite size, λ is the X-ray wavelength and C is the correction factor taken as 0.90 in the calculation.

The calculated value of the crystallite sizes varies between 53 to 69 nm when Co$_3$O$_4$ film annealed between 400˚C to 700˚C. It was observed that crystallite size increased with increasing annealing temperature, which can be understood by considering the merging process induced from thermal annealing. For Co$_3$O$_4$ nanoparticles, there are many dangling bonds related to the cobalt of

oxygen defects at the grain boundaries. As a result, these defects are favorable to the merging process to form larger Co$_3$O$_4$ grains while increasing the annealing temperature. The FWHM of (311) plane of Co$_3$O$_4$ thin film with various annealing temperatures is also compared. As the annealing temperature increases from 400˚C - 700˚C, the FWHM value of Co$_3$O$_4$ thin film exhibits a tendency to decrease, which can be attributed to the coalescences of grains at higher annealing temperature [14]. As a result, it implies that the crystallinity of the Co$_3$O$_4$ thin films is improved at higher annealing temperatures. Other workers [11,12] have also observed the improvement in crystallinity of the Co$_3$O$_4$ thin films with the increase of annealing temperature. These may be due to high annealing temperature providing energy to crystallites gaining enough energy to orient in proper equilibrium sites, resulting in the improvement of crystallinity and degree of orientation of the Co$_3$O$_4$ films.

3.3. Surface Morphological Studies

Figure 3 shows SEM images of cobalt oxide thin film annealed at 400˚C - 700˚C. Figure shows the nearly same surface morphology for all films with slight increase in grain size .The film surface looks smooth and composed of very fine elongated particles smaller than 80 nm in length connected by two-three spherical grains of about 40 nm - 45 nm in diameters. From SEM image, overgrowth of clusters is clearly seen. Initially grown nanograins may have increased their size by further deposition and come closer to each other. The cobalt oxide film surface is well covered without any pinholes and cracks. Such surface morphology may offer increased surface area, feasible for super capacitor and gas sensing application [15].

3.4. Electrical Properties

3.4.1. DC Conductivity Measurement
The four-probe technique was employed for measurement of variation of dark electrical conductivity of Co$_3$O$_4$ film with annealing temperature. The variation of log σ with reciprocal temperature (1000/T) is depicted in **Figure 4**. After annealing, room temperature electrical conductivity was increased from 10^{-4} to 10^{-2}·(Ω cm)$^{-1}$, due to

increase in the crystallite size and reduced scattering at the grain boundary. Similar type of increase in electrical conductivity for sprayed cobalt oxide has been observed by Patil *et al*. [16].

From **Figure 4** it is observed that the conductivity of film is increases with increase in annealing temperature, further it is observed that conductivity obeys Arrhenius behavior indicating a semiconducting transport behavior. The activation energies were calculated using the relation:

$$\sigma = \sigma_o \exp\left(-E_a/kT\right) \qquad (3)$$

where, σ is the conductivity at temperature T, σ_o is a constant, k is the Boltzmann constant, T is the absolute temperature and E_a is the activation energy. The activetion energy represents the location of trap levels below the conduction band. From **Figure 4**, it is seen that the acti-

vation energy (HT) is increases from 0.21 eV, to 0.54 eV, when film annealed between 400˚C - 700˚C indicating no significant change.

3.4.2. Thermoelectric Power Measurement

The thermo-emf of Co_3O_4 films annealed between 400˚C - 700˚C was measured as a function of temperature in the temperature range 300 K - 500 K. The polarity of the thermally generated voltage at the hot end was negative, indicating that the Co_3O_4 films are of p-type [15]. The variation of the thermo-emf (ΔV) with temperature is shown in **Figure 5**. The thermo-emf increases with increasing temperature. The thermo-electric power (TEP) was used to evaluate the carrier mobility (μ) and carrier concentration (n) using the relation,
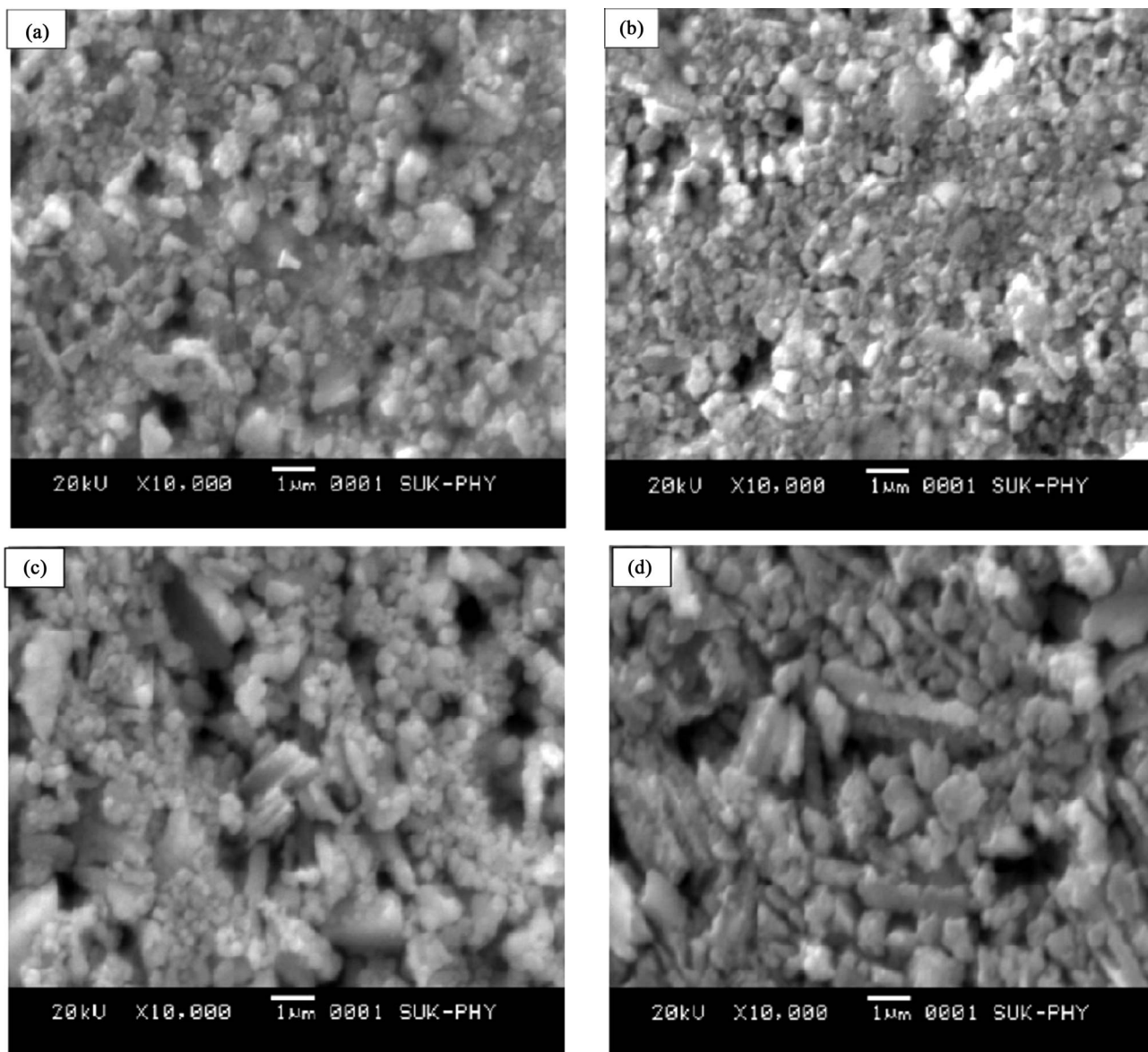

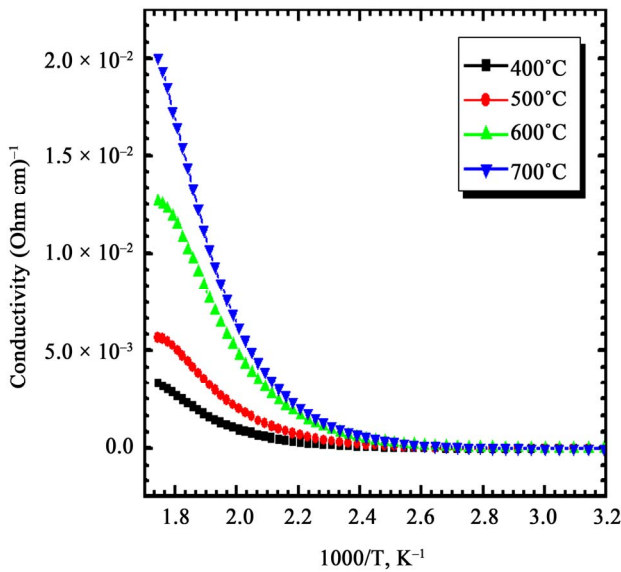**Figure 3. SEM of Co₃O₄thin films anneled at (a) 400˚C, (b) 500˚C, (c) 600˚C and (d) 700˚C.**

Figure 4. Arrhenius plot of dc conductivity vs. 1000/T of Co₃O₄ thin films annealed at different temperatures.
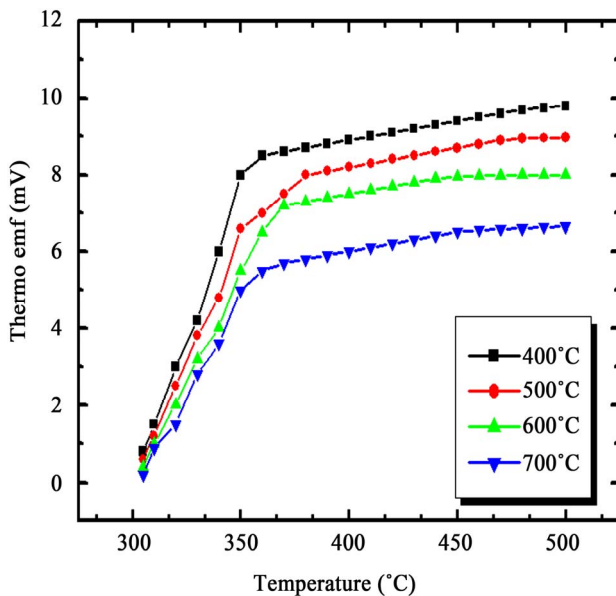

Figure 5. The variation of thermo-emf with temperature for of Co₃O₄ thin films annealed at different temperatures.

$$TEP = -k/eA + \ln\left[2\left(2\pi\, m_c^* kT\right)^{3/2}\big/nh^3\right] \quad (4)$$

where A is a thermoelectric factor (2 for cobalt oxide), n is electron density, h is Plank's constant, m_c^* is the effective mass of the electron.

After substitution of various constants Equation (4) simplifies to [17]

$$Log\, n = 3/2 \log T - 0.005 TEP + 15.719 \quad (5)$$

The electron density (n) was calculated using the above equation and was in the order of 10^{19} cm^{-3} for films an-

nealed at 400°C - 700°C. The mobility (µ) of the charge carriers is determined from the relation,

$$\mu = \sigma/ne \quad (6)$$

where n is electron density and σ is conductivity. The variation of log n and log µ as a function of temperature for Co₃O₄ film annealed at 700°C is shown in **Figure 6**. It is observed that electron density (n) and mobility (µ) increases with temperature. The electron carrier concentration (n) and mobility (µ)were estimated to be of the order of 2.4 to 4.5 × 10^{19} cm^{-3} and 5.2 to7.0 × 10^{-5} cm^2·V^{-1} respectively for films annealed between 400°C to 700°C. The temperature variation of carrier mobility suggests that there is a considerable amount of scattering mechanism due to the intergrain barrier potential [18-21]. This carrier scattering is temperature dependent, and therefore it is related to the carrier mobility (µ) and intergranular potential $\left(\Phi_b\right)$ [18-21].

$$\mu = \mu_o \exp\left(-\Phi_b/kT\right) \quad (7)$$

where all the terms have their usual meanings. Intergranular potential (scattering potential) is therefore calculated from the log µ versus 1000/T variation as suggested by Micocci *et al.* [20] and its typical value is 0.2 eV for Co₃O₄ film annealed at 700°C.

3.5. Optical Studies

The Co₃O₄ thin films on glass substrate were used to study the optical absorption. The optical absorption of Co₃O₄ thin films in the wavelength range of 200 nm - 1000 nm has been investigated.

Figure 7 shows plots of $\left(\alpha h\nu\right)^2$ as a function of photon energy (hν) for Co₃O₄ thin films as a function annealing temperature (400°C - 700°C). Since the plots are almost linear, the direct nature of the optical transition in Co₃O₄ is confirmed. Extrapolation of these curves to photon en-
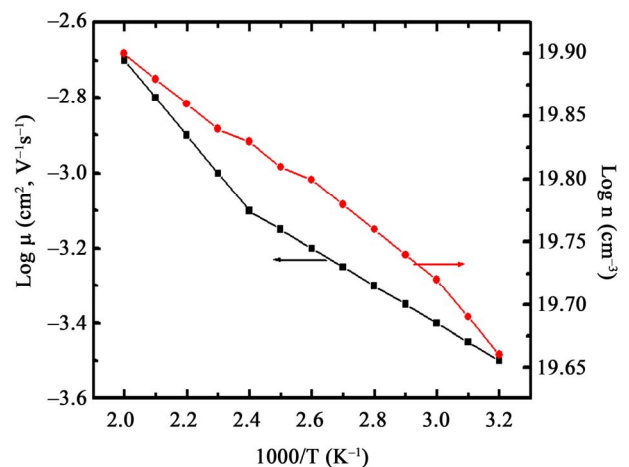

Figure 6. Variation of log n and log µ as a function of temperature for Co₃O₄ thin films annealed at 700°C.

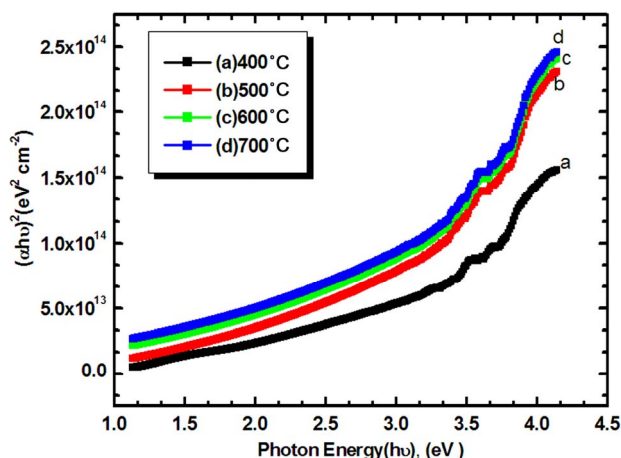**Figure 7. Plot of $(\alpha h\upsilon)^2$ versus $(h\upsilon)$ of Co_3O_4 thin films for different annealing temperatures.**

ergy axis reveals the band gaps. The optical absorption data were analyzed using the following classical relation for near edge optical absorption in semiconductor.

$$\alpha = \alpha_o \left(h\nu - E_g \right)^n \Big/ h\nu \qquad (8)$$

where "α_o" is a constant, "E_g" is the semiconductor band gap and "n" is a number equal to 1/2 for direct gap and 2 for indirect gap compound.

The band gap of Co_3O_4 film was found to be decreased from 2.58 to 2.07 eV for films annealed at 400˚C - 700˚C. Patil *et al.* [22] and Khandalkar *et al.* [20] reported the slightly lower band gaps 2.04 eV and 1.95 eV for as-prepared Co_3O_4 thin films [23]. The decrease in E_g with annealing temperature could be due to increase in crystalline size and reduction of defect sites. This is in good agreement with the experimental results of XRD analysis. According to XRD results, the mean grain size has increased with increased annealing temperature. As the grain size has increased, the grain boundary density of a film decreased, subsequently, the scattering of carriers at grain boundaries has decreased [24]. A continuous increase of optical constants (α and E_g) and also the shift in absorption edge to a higher wavelength with increasing annealing temperature may be attributed to increase in the particle size of the crystallites along with reduction in porosity.

The decrease in optical band gap energy is generally observed in the annealed direct-transition-type semiconductor films. Hong *et al.* [25] observed a shift in optical band gap of ZnO thin films from $3\cdot31$ eV - $3\cdot26$ eV after annealing, and attributed this shift to the increase of the ZnO grain size. Chaparro *et al.* [26] ascribed this 'red shift' in the energy gap, E_g, to an increase in crystallite size for the annealed ZnSe films. Bao and Yao [27] also reported a decrease in E_g with increasing annealing temperature for $SrTiO_3$ thin films, and suggested that a shift of the energy gap was mainly due to both the quantum-

size effect and the existence of an amorphous phase in thin films. In present case, the mean crystallite size increases from 53 nm to 69 nm after annealing from 400˚C - 700˚C. Moreover, it is understood that the amorphous phase is reduced with increasing annealing temperature, since more energy is supplied for crystallite growth, thus resulting in an improvement in crystallinity of Co_3O_4 films. Therefore, it is believed that both the increase in crystallite size and the reduction in amorphous phase cause are decreasing in band gap of annealed Co_3O_4 films. The change in optical band gap energy, E_g, reveals the impact of annealing on optical properties of the Co_3O_4 films.

4. Conclusions

Thin films of nanocrystalline cobalt oxide were prepared by low-cost sol gel spin coating technique. The Co_3O_4 films were annealed for various temperatures between 400˚C to 700˚C. The XRD results revealed that the Co_3O_4 thin film has a good nanocrystalline spinal structure. Nanocrystalline grains with some overgrown clusters of cobalt oxide were reveled from surface morphological studies. The dc electrical conductivity is increased from 10^{-4} to 10^{-2} $(\Omega \cdot cm)^{-1}$ for films annealed at 400˚C - 700˚C. The P-type electrical conductivity is confirmed from thermo-emf measurement with no appreciable change in thermoelectric power after annealing. The electron carrier concentration and mobility of Co_3O_4 films annealed at 400˚C - 700˚C were estimated to be of the order of 2.4 to 4.5×10^{19} cm^{-3} and 5.2 to 7.0×10^{-5} $cm^2 \cdot V^{-1} \cdot s^{-1}$ respectively. Optical absorption studies show low-absorbance in IR and visible region with band gap 2.58 eV (at 400˚C) which was decreased to 2.07 eV (at 700˚C). This has been attributed to the decrease in defect levels.

5. Acknowledgments

REFERENCES

[1] A. O. Gulino, P. Dapporto, P. Rossi and I. Fragalà, "Novel Self-Generating Liquid MOCVD Precursor for Co_3O_4 Thin Films," *Chemistry of Materials*, Vol. 15, No. 20, 2003, pp. 3748-3752. doi:10.1021/cm034305z

[2] S. G. Kandalkar, C. D. Lokhande, R. S. Mane and S. H. Han, "Preparation of Cobalt Oxide Thin Films and Its Use in Supercapacitor Application," *Applied Surface Science*, Vol. 254, No. 17, 2008, pp. 5540-5544. doi:10.1016/j.apsusc.2008.02.163

[3] Y. Chen, Y. Zhang and S. Fu, "Synthesis and Characteri-

SNL

zation of Co_3O_4 Hollow Spheres," *Materials Letters*, Vol. 61, No. 3, 2007, pp. 701-705. doi:10.1016/j.matlet.2006.05.046

[4] Y. Dong, K. He, L. Yin and A. Zhang, "A Facile Route to Controlled Synthesis of Co_3O_4 Nanoparticles and Their Environmental Catalytic Properties," *Nanotechnology*, Vol. 18, No. 43, 2007, pp. 435602-435608. doi:10.1088/0957-4484/18/43/435602

[5] X. W. Lou, D. Deng. J. Y. Lee, J. Feng and L. A. Archer, "Self-Supported Formation of Needlelike Co_3O_4 Nanotubes and Their Application as Lithium-Ion Batteries Electrodes," *Advanced Materials*, Vol. 20, No. 2, 2008, pp. 258-262.

[6] S. Lian, E. Wang, L. Gao and L. Xu, "Fabrication of Single-Crystalline Co_3O_4 Nanorods via a Low-Temperature Solvothermal Process," *Materials Letters*, Vol. 61, No. 18, 2007, pp. 3893-3896. doi:10.1016/j.matlet.2006.12.052

[7] D. Zou, C. Xu, H. Luo, L. Wang and T. I. Ying, "Synthesis of Co_3O_4 Nanoparticles via an Ionic Liquid-Assisted Methodology at Room Temperature," *Materials Letters*, Vol. 62, Vol. 12-13, 2008, pp. 1976-1978.

[8] P. Poizot, S. Laruelle, S. Grugeon, L. Dupont and J. M. Tarascon, "Nano-Sized Transition-Metal Oxides as Negative-Electrode Materials for Lithium-Ion Batteries," *Nature*, Vol. 407, No. 6803, 2000, pp. 496-499.

[9] B. Varghese, T. C. Hoong, Y. W. Zhu, M. V. Reddy, V. R. Chowdari, T. S. Wee, B. C. Vincent, C. T. Lim and C. Sow, "Co_3O_4 Nanostructures with Different Morphologies and Their Field-Emission Properties," *General & Introductory Materials Science*, Vol. 17, No. 12, 2007, pp. 1932-1939. doi:10.1002/adfm.200700038

[10] J. Jiang, L.-C. Li, "Synthesis of Sphere-Like Co_3O_4 Nanocrystals via a Simple Polyol Route," *Materials Letters*, Vol. 61, No. 27, 2007, pp. 4894-4896. doi:10.1016/j.matlet.2007.03.067

[11] J. Gao, Y. Zhao, W. Yang, J. Tian, F. Guan and Y. Ma, "Sol Gel Synthesis of Co_3O_4," *Journal of University of Science and Technology Beijing*, Vol. 10, No. 1, 2003, pp. 54-57.

[12] H. Shim, V. R. Shinde, H. Kim, Y. Sung and W. Kim, "Porous Cobalt Oxide Thin Films from Low Temperature Solution Phase Synthesis for Electrochromic Electrode," *Thin Solid Films*, Vol. 516, No. 23, pp. 8573-8578. doi:10.1016/j.tsf.2008.05.055

[13] L. Pan and Z. Zhang "Prepartion, Electrocatalytic and Photocatalytic Performances of Nanoscised CuO/Co_3O_4 Composite Oxides," *Journal of Materials Science*: *Materials in Electronics*, Vol. 21, No. 12, 2010. pp. 1262-1269. doi:10.1007/s10854-010-0059-1

[14] V. Gupta and A. Mansingh, "Influence of Post-Deposition Annealing on the Structural and Optical Properties of Sputtered Zinc Oxide Film," *Journal of Applied Physics*, Vol. 80, No. 2, 1996, pp. 1063-1073. doi:10.1063/1.362842

[15] T. P. Gujar, V. R. Shinde, C. D. Lokhande, R. S. Mane and S.-H. Han, "Bismuth Oxide Thin Films Prepared by Chemical Bath Deposition (CBD) Method: Annealing Ef-

fect," *Applied Surface Science*, Vol. 250, No. 1-4, 2005, pp. 161-167. doi:10.1016/j.apsusc.2004.12.050

[16] S. G. Pawar, S. L. Patil, M. A. Chougule and V. B. Patil, "Synthesis and Characterization of Nanocrystalline TiO_2 Thin Films," *Journal of Materials Science*: *Materials in Electronics*, Vol. 22, No. 3, 2011, pp. 260-264. doi:10.1007/s10854-010-0125-8

[17] R. R. Heikes and R. W. Ure, "Thermoelectricity Science and Engineering," lnster Science, New York, 1961.

[18] V. B. Patil, S. G. Pawar, S. L. Patil, "ZnO Nanocrystalline Thin Films: A Correlation of Microstructural, Optoelectronic Properties," *Journal of Materials Science*: *Materials in Electronics*, Vol. 21, No. 4, 2010, pp. 355-359. doi:10.1007/s10854-009-9920-5

[19] R. L. Petriz, "Barrier Theory of the Photoconductivity of Lead Sulfide," *Physical Review*, Vol. 104, 1956, pp. 1508-1516.

[20] G. Micocci, A. Tepore, R. Rella and O. P. Sicilian, "Electrical and Optical Characterization of Electron Beam Evaporated In_2Se_3 Thin Films," *Physica Status Solidi* (*a*), Vol. 148, No. 2, 1995, pp. 431-438. doi:10.1002/pssa.2211480211

[21] F. B. Michehti and P. Mark, "Effect of Chemisorbed Oxygen on the Electrical Properties of Chemically Sprayed CdS Thin Films," *Applied Physics Letters*, Vol. 10, No. 4, 1967, pp. 136-140. doi:10.1063/1.1754881

[22] P. S. Patil, L. D. Kadam, C. D. Lokhande, "Preparation and Characterization of Spray Pyrolysed Cobalt Oxide Thin Films," *Thin Solid Films*, Vol. 272, No. 1, 1996, pp. 29-32. doi:10.1016/0040-6090(95)06907-0

[23] S. G. Khandalkar, J. L. Gunjalkar, C. D. Lokhande and O.-S. Joo, "Synthesis of Cobalt Oxide Interconnected Flackes and Nano-Worms Structures Using Low Temperature Chemical Bath Deposition," *Journal of Alloys and Compounds*, Vol. 478, No. 1-2, 2009, pp. 594-598. doi:10.1016/j.jallcom.2008.11.095

[24] J. H. Lee, K. H. Ko and B. O. Park, "Electrical and Optical Properties of ZnO Transparent Conducting Films by the Sol-Gel Method," *Journal of Crystal Growth*, Vol. 247, No. 1-2, 2003, pp. 119-125. doi:10.1016/S0022-0248(02)01907-3

[25] R.-J. Hong, J.-B. Huang, H.-B. He, Z.-X. Fan and J.-D. Shao "Influence of Different Post-Treatments on the Structure and Optical Properties of Zinc Oxide Thin Films," *Applied Surface Science*, Vol. 242, No. 3-4, 2005, pp. 346-352. doi:10.1016/j.apsusc.2004.08.037

[26] A. M. Chaparro, M. A. Martinez, C. Guillen, R. Bayon, M. T. Gutierrez and J. Herrero, "SnO_2 Substrate Effects on the Morphology and Composition of Chemical Bath Deposited ZnSe Thin Films," *Thin Solid Films*, Vol. 361-362, No. 1-2, 2000, pp. 177-182. doi:10.1016/S0040-6090(99)00791-9

[27] D.-H. Bao, X. Yao, N. Wakiya, K. Shinozaki and N. Mizutani, "Band-Gap Energies of Sol-Gel-Derived $SrTiO_3$ Thin Films," *Applied Physics Letters*, Vol. 79, No. 23, 2001, pp. 3767-3772. doi:10.1063/1.1423788